International Society for Rock Mechanics and Rock Engineering
Norwegian Group for Rock Mechanics

ISRM International Symposium
Eurock 2025 – Expanding the Underground Space
Trondheim, Norway, 16-20 June
ISBN 978-82-8208-079-8

Fragmentation patterns during rockfall: analysis of the influence of discontinuities and impact conditions through drop tests

M. Marchelli
Department of Environment, Land and Infrastructure Engineering, Politecnico di Torino, Turin, Italy
maddalena.marchelli@polito.it

D. E. Guccione, A. Giacomini, O. Buzzi
Centre for Geotechnical Science and Engineering, The University of Newcastle, Callaghan, NSW 2308, Australia

Abstract

Fragmentation of rock blocks upon impacts is frequently observed during rockfall. The increase in frequency of rockfall events due to climate change makes fundamental the knowledge and prediction of possible blocks fragmentation to assess and manage the risk. Although fragmentation occurs regularly and at various scales, the process has not been completely investigated in rockfall. In this specific field, the term fragmentation describes the division of an initial block by either breakage, generating new pieces, or the disaggregation of the blocks delimited by fracture stuck together thanks to a small cohesion or some kind of cementation, or even both phenomena together.

Fragmentation of brittle spheres, made of mortar, has been studied experimentally and numerically by some of the Authors through vertical drop tests performed in a fragmentation cell conceived and built at the University of Newcastle. Interesting findings on the breakage of intact rock at a meso-scale level have been revealed and published.

The present work deals with an experimental campaign in which discontinuities were created into the mortar spheres. To this aim, a specific specimen assembly technique was adopted. The mortar spheres were casted in separate parts and then glued together with mortar with lower mechanical performances. Different discontinuity patterns were investigated, considering how the position and inclination with respect to the impacted surface affect the fragmentation mechanisms. The generated patterns were studied by detailed image analyses, and they were related to discontinuities' geometry and impact conditions.

Interestingly, the number of hemispherical fractures, when formed, together with the presence of secondary cracks, is strongly related to all the parameters. In specific conditions, disaggregation only occurs. Knowing the state of the rock face and possible released blocks, the results can provide interesting insights on the number and type of possible fragments.

Keywords

Fragmental rockfall, fracture pattern, rock joints, drop tests.

ISRM

NBG

1 Introduction

Of all natural hazards of landslide type, rockfall is particularly dangerous, potentially affecting people, structures and infrastructures (Scavia et al., 2020). Due to the involved effects, e.g. fatalities, structural damages, and interruption of traffic and activities, the deep knowledge and prediction of these events represent a crucial issue to properly manage the risk. The forecast of blocks trajectories together with their kinematic parameters is fundamental to manage the risk and predispose effective mitigation measures (Crosta et al., 2015). During rockfall events, fragmentation of rock blocks upon impacts is commonly observed (Corominas et al., 2017). In this context, fragmentation refers to either the breakage of an initial block into new pieces, or the disaggregation of blocks delimited by fractures (joints) held together by small cohesion or cementation, or even both phenomena occurring simultaneously (Hungr 1988; Corominas et al. 2019). Despite diffusely present in nature and across various scales, fragmentation process in rockfall has not been fully studied yet. Field tests (Giacomini et al., 2008; Gili et al., 2022), laboratory tests (Ye at al, 2019; Lin et al., 2020; Guccione et al., 2023), and numerical investigations (Wittel et al., 2008; Wang and Tonon, 2011; Ye et al., 2020) have indicated that the shape of the block, its impacting angle, the presence of discontinuities and their orientation at impact, the impact velocity, together with the characteristics of the impacted soil affect fragmentation occurrence and pattern. Referring to the breakage case, only, i.e. intact rock, several laboratory and numerical (Tomas et al., 1999; Khanal et al., 2004; Wu et al., 2004; Wittel et al., 2008, Guccione et al., 2021a) studies on rocklike brittle materials have been conducted, individuating the major fracture patterns. These studies offer important insights into the phenomenon, while a universal fragmentation model and a comprehensive predictive trajectory model for fragmental rockfall is still missing. The existing fragmentation models (Ruiz-Carulla et al., 2017; Marchelli and De Biagi, 2019) generally require site-specific parameters that must be calibrated case by case. Similarly, the existing fragmentation trajectory models, generally implemented on a lumped-mass framework, need several parameters that can prove difficult to determine (Matas et al., 2020, Frattini et al., 2012; Matas et al., 2020; Lanfranconi et al., 2024). The fact that fragments kinematic post impact is handled stochastically reflects the current knowledge gap on the topic and the effects of discontinuities have not been properly tackled yet.

The present work deals with fragmental rockfalls due to disaggregation, aiming at individuating the possible fracture patterns and their occurrence according to the position of a discontinuity inside the block, its inclination with respect to the impacted surface, and the impact velocity. To achieve such goal, vertical drop tests of brittle mortar spheres with discontinuities were conducted using the fragmentation cell designed and prototyped at the University of Newcastle, Australia (Guccione et al., 2021b). The discontinuities were introduced using a specific specimen assembly technique: the spheres were cast in separate parts and then glued together with a lower-performance mortar in terms of mechanical resistance. Two different discontinuity patterns were considered, i.e. in the center or at ¼ of the sample, simulating different position inside a rock block. The samples were dropped at different heights and with different orientation in reference to the discontinuity, obtaining different impact velocities and inclination of the discontinuity in reference to the impacted surface. Detailed image analyses were performed, and a classification of the possible fracture patterns was firstly proposed. The influence of all the variables on the occurrence of each pattern was analysed and interesting findings were highlighted. In the following, Sec. 2 reports the methodology of the tests, Sec. 3 the proposed classification, Sec. 4 the results are discussed evaluating the influence of the different variables. Finally, conclusions and future perspective are outlined.

2 Experimental methods

The goal of the study was to investigate the fracture modes of the brittle sphere and how the fragmentation pattern is affected by the number, position and orientation at impact of discontinuities. In the present study, a total of 154 mortar samples were prepared, dropped and analysed. The choice of a fixed shape, i.e. spherical, and a fixed material, i.e. mortar, was driven by the desire to mitigate the effects of impact variability in natural rocks and to control the effects of selected variables, only. For the same reason all the samples have the same diameter, i.e. 100 mm. The mortar was made of silica sand, Portland cement, hydrated lime and water, with a proportion of 3:1:0.125:1 by mass, respectively. Cement accelerant was added (2% by weight of cement weight) to fasten the curing. As all the samples were cast in different batches, a series of material characterisation tests (Brazilian tests (BT), unconfined compressive tests (UCS), and toughness tests, ISRM 1978, 1979, Kuruppu et al., 2014, respectively) were conducted for each batch a material. A total of 66 BT, 64 UCS and 72 toughness tests were performed, yielding a mean tensile strength of 1.92 (±0.20) MPa, a uniaxial compressive resistance of 16.87 (±2.61) MPa, an elastic modulus of 2103 (±91) MPa, and a fracture toughness of 0.416 (±0.095) MPa·m$^{1/2}$. To simulate rock discontinuities, generally unfilled or soil-infilled (sometimes with a small consolidation), a different mortar type of approximately half the strength of the one used for the sphere, was used. For the discontinuities, the proportion of sand, cement, hydrated lime and water are 3.5:0.8:1:1.2 (by mass), respectively. The 33 BT, 30 UCS, and 38 toughness tests gave a mean tensile strength of 0.97 (±0.19) MPa, a uniaxial compressive resistance of 7.65 (±1.75) MPa, an elastic modulus of 1202 (±134) MPa, and a fracture toughness of 0.190 (±0.031) MPa·m$^{1/2}$. The spheres were cast in 3D-printed moulds made of high-density Acrynitrile Butadiene Styrene (Fig. 1a). To create the discontinuities, the different portions of spheres were first created and then glued together. To obtain a homogeneous infill for all the spheres, a minimum thickness of 2 mm was attempted, with a maximum of 4 mm. Once prepared, the spheres were left to cure for 2 weeks in a 100% humid environment (fog room) and 3 weeks in an oven set at 40°.

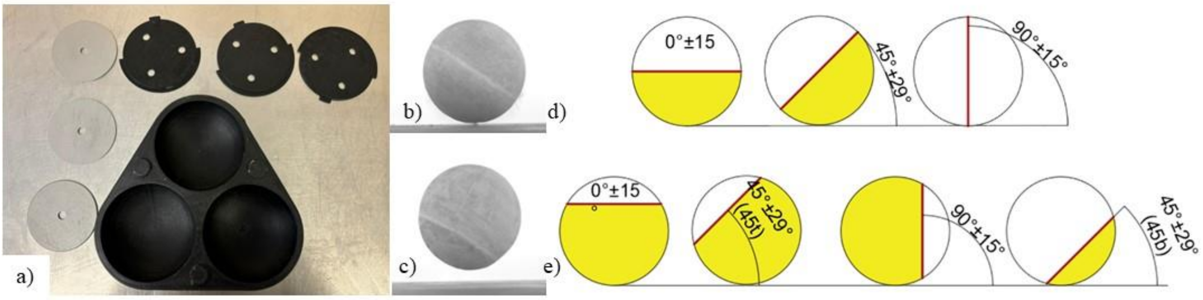

Fig. 1 a) High-density Acrynitrile Butadiene Styrene moulds and discs used to create partitions in the sphere, b) 1-2D sphere (i.e. discontinuity in the middle of the sphere), c) 1-4D sphere (i.e. discontinuity at ¼ of the sphere diameter), d) impact positions for 1-2D, e) impact positions for 1-4D. In d) and e) a yellow area highlights the zone in which the impact can occur, and a red line highlights the position of the discontinuity.

To study the effects of the position of the discontinuity inside the rock block on the fragmentation pattern upon impact, two discontinuity configurations were investigated: a single discontinuity in the middle of the sphere (specimens referred to as 1-2D) and a single discontinuity at ¼ of the diameter (referred to as 1-4D) (Fig. 1b, c). To perform the drop tests, different orientations of the discontinuities with respect to the impacted surface (slab) were considered, together with different impact velocities. For the 1-2D, 5, 6, 7, 8.5, and 10 m/s were performed, while 6, 7 and 10 m/s for the 1-4D. The selected velocities were chosen considering that for spheres of equal diameter but without discontinuities, according to Guccione et al. (2021a), the same impact velocities correspond to a not-fracturing (survival) probability of 90%, 57%, 4%, 0%, and 0% for 5, 6, 7, 8.5, and 10 m/s, respectively. As detailed in Sec. 4, the inclinations of the discontinuity in reference to the slab, named herein as “impact position”, were been grouped in 3 (for 1-2D) and 4 (for 1-4D) categories, i.e. 0°±15°, 45°±29°, and 90°±15° for the 1-2D and 0°±15°, 45b°±29°, 90°±15°, 45t°±29° (Fig. 1d, e). To ease the notation, from here on, each impact position is recalled as the mean angle between the discontinuity and the slab, only (hence neglecting the range). For the 1-4D 45° case, the letters *b* and *t* stand for “bottom” and “top” and refer to the position of the discontinuity with respect to the impact surface, as highlighted in Fig. 1e. All the performed tests were summarized in Table 1. As the drop was not guided, i.e. the sample is free to fall, due to some small asymmetries of the samples an equal number of tests per each impact group was not achieved. Moreover, where the tolerance in the impact position is large, e.g. 45°±29° in 1-2D, a higher number of samples was investigated.

The facility in which tests were performed, called fragmentation cell, consists of an enclosed hexagonal container including an instrumented concrete slab (three load cells of 100 kN capacity each, two accelerometers of 50 g capacity), a release system using vacuum, and a system of image recording devices composed by 4 synchronised Optronics CR600 × 2 and 2 Phantom VEO-E340L high-speed cameras, positioned outside the cell. Additional LED strips, LED panels and LED spotlights were also mounted inside the cell for having an optimal contrast for the collection of images at 500 fps for all the cameras, and 500 µs (for Optronics cameras) and 100 µs (for Phantom cameras) exposure time (refer to Guccione et al., 2021b for details). All the images of the free-falling spheres, the rebounds following impact and motion of the sphere alone or the of fragments eventually created were recorded by the high-speed cameras and analysed to understand the possible fracture patterns.

Table 1 Summary of the performed drop tests

	1-2D											
Velocity		**6 m/s**			**7 m/s**			**8.5 m/s**			**10 m/s**	
Position	**0°**	**45°**	**90°**	**0°**	**45°**	**90°**	**0°**	**45°**	**90°**	**0°**	**45°**	**90°**
N° of samples	8	7	7	6	9	7	2	11	2	5	6	9
Total n° of samples		**22**			**22**			**15**			**20**	

	1-4D											
Velocity		**6 m/s**				**7 m/s**				**10 m/s**		
Position	**0°**	**45°b**	**90°**	**45°t**	**0°**	**45°b**	**90°**	**45°t**	**0°**	**45°b**	**90°**	**45°t**
N° of samples	5	7	6	6	3	11	5	6	4	12	5	5
Total n° of samples		**24**				**25**				**26**		

3 Fracture pattern classification

The high-quality images obtained for each test were analysed to identify if common fracture patterns emerge and how impact conditions and the discontinuity configuration affect the fragmentation pattern. In the following, the observed patterns and the proposed nomenclature are listed. In cases in which the influence of the discontinuity is negligible, the proposed fracture modes follow the findings of previous studies (Tomas et al., 1999; Wu et al., 2004; Khanal et al., 2004; Wu et al., 2006; Wittel et al., 2008; Carmona et al., 2008, Guccione et al., 2023), which have also highlighted the influence of the impact energy on damages or fragmentation occurrence. Note that when a fracture forms along the discontinuity, we do not distinguish if it is within the filling or along the interface between the two mortars.

3.1 Spheres without discontinuity or without discontinuity influence

In a sample without discontinuity or discontinuity influence, and for low impact energies, one or more meridian cracks that extend above the contact point of the sample and follow the direction of the impact can generally be seen. As the energy increases, some of the meridian cracks reach the top free surface of the sphere, fragmenting the material into typically two to four wedge-shaped fragments. If more fragments are formed, they resemble “orange slices”. Meridian cracks are therefore referred to as primary cracks. Further increasing the energy, secondary oblique plane cracks form, as a result of the inertia forces (Tomas et al., 1999), further breaking up the already formed fragments into wedge-shaped smaller pieces. At the specimen-target contact point circular cracks generate together with convergent shear cracks resulting in a cone-shaped fragment. Increasing the energy, due to further crack propagation and dispersion, a top cone of different size can be observed.

The fragmentation patterns are hence classified as: (i) meridian (M), when a unique meridian fracture occurs and the sphere splits in a tensile mode (Fig. 2a); (ii) orange slices (O), when multiple meridian fractures occur with possibility of secondary oblique plane cracks (not in correspondence of the discontinuities) (Fig. 2b); (iii) orange slices with top cone (OTC), when a significant top cone fragment is formed, together with a bottom cone, i.e. cracks follow the trajectory of a convergent cone (Fig. 2c). While in the O case the created fragments look like orange slices or, in case of oblique cracks, wedges; in the OTC case, “lune-shaped” fragments arise around the cone.

3.2 Spheres with one or more discontinuities

When the presence of one or more discontinuities affect the fragmentation pattern, the following patterns were observed and proposed: (i) parallel disaggregation (PD) if the sphere separates along the discontinuities only (Fig. 2d); (ii) meridian & parallel disaggregation (M+PD), when a unique meridian fracture starts at the slab-sphere impact point, but fractures also occur along discontinuities (Fig. 2e); (iii) orange slices & parallel disaggregation (O+PD), when meridian fractures start at slab-sphere impact point, but fractures also occur along discontinuities (Fig. 2f,g); (iv) orange slices with top cone & parallel disaggregation (OTC+PD), when a significant top cone fragment is formed together with lune-shaped fragments, but fractures also occur along discontinuities (Fig. 2h). For M+PD, O+PD and OTC+PD, according to the impact position with respect to the discontinuity/ies, the position of the discontinuity in the block, and the impact velocity: (a) meridian crack(s) and parallel disaggregation can both occur completely, or (b) either meridian (c) or parallel disaggregation, (d) or both can be incomplete.

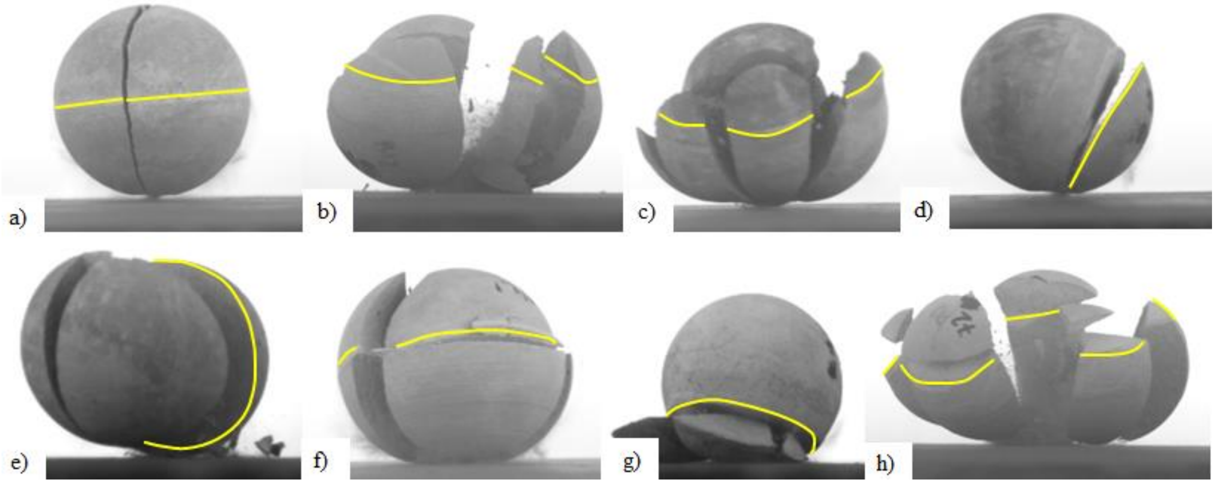

Fig. 2 Illustration of the observed fragmentation patterns: a) M in a 1-2D case; b) O in a 1-4D case; c) OTC in a 1-4D case; d) PD in a 1-4D; e) M+PD: incomplete M and complete parallel disaggregation in a 1-2D case; f) O+PD: complete orange slices and incomplete parallel disaggregation in a 1-2D case, g) O+PD: incomplete orange slices and complete parallel disaggregation in 1-4D case, e) OTC+PD: complete OTC and incomplete PD in a 1-4D case. All the photos are in front view. A yellow line highlights the position of the discontinuity.

4 Results and discussion

The obtained data were analysed considering not only the differing impact velocities but also the impact position. As in rockfall trajectory analysis, among the predicted quantities, the impact velocity is that with less uncertainties, results were first grouped according to impact velocity and then according to the impact position. Fig. 3 and Fig. 4 report the frequency of each possible fracture pattern for the 1-2D and the 1-4D tests, respectively. It should be recalled that not the same number of tests were performed for each impact velocity.

Starting from the 1-2D configuration, Table 2 reports the percentage of the sample survived at the impact. As expected, the higher the impact velocity, the lower the survival probability. This observation is exacerbated when the impact occurs near or directly on the discontinuity. For 0°, the influence of the discontinuity seems to be negligible up to 7 m/s, where cases with a meridian crack only (M) can be observed. For the velocity range here investigated, some general considerations can be drawn:

- if the impact point lies on the discontinuity, i.e. at an angle of 90°, fragmentation occurs along the discontinuity, and all the fracture patterns display a complete parallel disaggregation.
- if the impact is not at 90° sharp but in the range of impact position 90°, also meridian cracks appear. For this position, a complete top cone pattern never displays.
- the formation of a top cone occurs only at the highest velocity for 0° and 45°, as its formation is related to high impact energies.
- at lower velocities, for the same impact positions, the occurrence of orange slices, combined with parallel disaggregation, is more frequent.

Considering 1-4D configuration, Table 2 shows the percentage of the sample survived at the impact. For most cases, an influence of the discontinuity is visible, as a unique O and 2 OTC (without PD case) occur for 0° and 10 m/s. Referring to the investigated velocities, it emerges:

- similarly to 1-2D but even more marked, M+PD failure mostly occurs at lower velocities, almost independently from the impact position, while for higher velocities O+PD failure (or even OTC+PD) failure prevails.
- parallel disaggregation occurs at all velocities, accompanied with an additional failure pattern if the collision does not occur on the discontinuity plan. Pure PD occurs when the impact is sharply on the discontinuity plane.
- the formation of a top cone occurs only for the highest investigated velocity (10 m/s) but for almost all the considered angles, even at 90°, except for 45b°. In this case, indeed, if the impact occurs below the discontinuity, single or multiple meridian cracks are observed

according to the impact velocity, with an increasing number of fractures as the kinetic energy increases, and the cracks stop at the discontinuity.

Table 2 Percentage of sample survived at the impact.

	1-2D											
Velocity	**6 m/s**			**7 m/s**			**8.5 m/s**			**10 m/s**		
Position	**0°**	**45°**	**90°**	**0°**	**45°**	**90°**	**0°**	**45°**	**90°**	**0°**	**45°**	**90°**
% of samples	100%	85%	0%	33%	11%	0%	0%	0%	0%	0%	0%	0%
Total % of samples	**63%**			**13%**			**0%**			**0%**		
	1-4D											
Velocity	**6 m/s**				**7 m/s**				**10 m/s**			
Position	**0°**	**45°b**	**90°**	**45°t**	**0°**	**45°b**	**90°**	**45°t**	**0°**	**45°b**	**90°**	**45°t**
% of samples	100%	71%	0%	100%	71%	0%	100%	71%	0%	100%	71%	0%
Total % of samples	**42%**				**24%**				**0%**			

For both 1-2D and 1-4D, the probability of formation of more primary and secondary cracks increases as the impact velocities increase. For all the considered velocities, there is the possibility that the sphere survives the impact if the velocity is smaller or equal to 7 m/s, for any discontinuity type, provided that the discontinuity angles are 0° or 45° (and 45t°). From images analysis, an interesting behaviour is observed when the impact position is 45° (or 45b° or 45t°). For 1-4D configuration with the smallest part close to the slab (45b° case), the impacted part completely fragments and the crack stops at the discontinuity (Fig. 2g). For 1-2D, the discontinuity influences the propagation of the cracks even though in some cases the parallel disaggregation in M+PD, O+PD and OTC+PD is just partial. For 1-4D configuration with the smallest part at the top (45t°), the discontinuity can, in some cases, not affect the fragmentation pattern (OTC), highlighting how the distance of the discontinuity plane with respect to the slab influence the pattern, too.

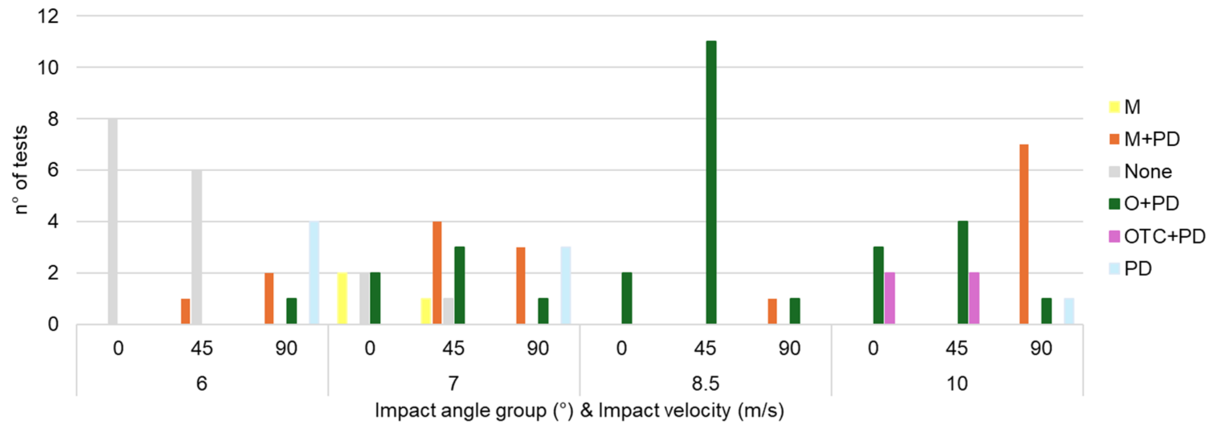

Fig. 3 Fracture patterns frequency grouped firstly for impact velocity and then for impact position for the 1-2D. “None” refers to not fragmented spheres.

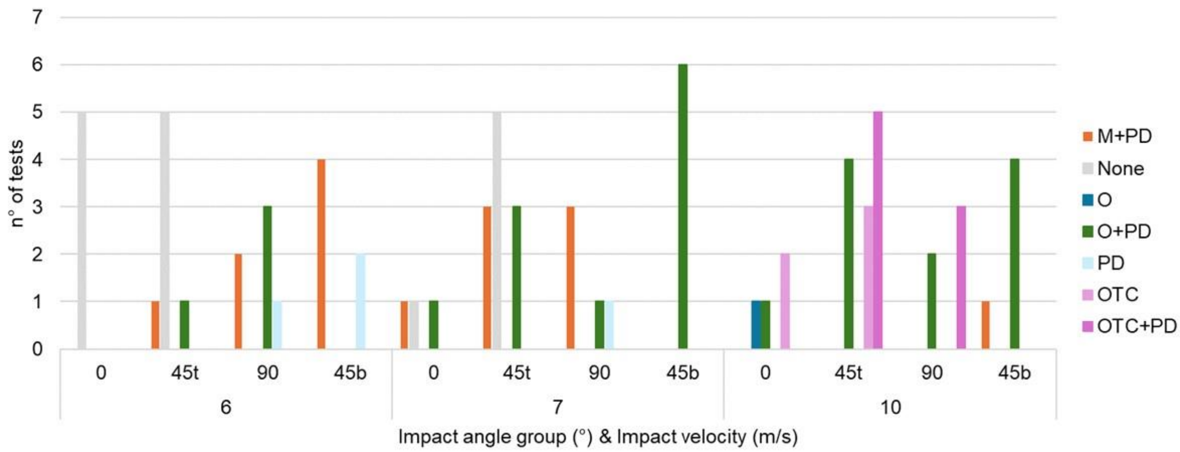

Fig. 4 Fracture patterns frequency grouped firstly for impact velocity and then for impact position for the 1-4D. “None” refers to not fragmented spheres.

5 Conclusions

This paper presents the results of a study on the influence of the discontinuities and impact conditions on the failure pattern of brittle material through drop tests. Mortar spherical samples colliding on a concrete slab were assumed representative of rock blocks masses impacting against a stiff surface. Different fracture patterns display, with a high influence of the discontinuity also at the lowest velocity, although the influence decreases when the impact position is 0°. The probability of formation of primary cracks increases increasing the impact velocity, while top cone appears at 10 m/s, only. The probability of fracture of the portion above the discontinuity does not only depend on the distance between the discontinuity plane and the slab but probably also on the surface area of the discontinuity itself. These results provide a useful information to understand the way of fracture of brittle material according to impact angle and velocity and to properly design mitigation measures (Marchelli et al., 2021). Further analyses will be done on other discontinuity patterns and on post-fracture fragments velocities.

Acknowledgements

This work was supported by Marie Curie Postdoctoral Fellowship 2022 (Call Horizon-MSCA-2022-PF-01, grant GA101103401 - RIDETHERISK project), by Australian Research Council (DP210101122 and IE230100410) and Rocscience Inc. The help received from Dr Michele Spadari, Elena Cozacenco and Wesley Murphey with preparing the samples and conducting the experiments is also gratefully acknowledged.

References

Carmona H. A., Wittel F. K., Kun F., & Herrmann H. J. (2008). Fragmentation processes in impact of spheres. Physical Review E—Statistical, Nonlinear, and Soft Matter Physics, 77(5), 051302. DOI 10.1103/PhysRevE.77.051302

Corominas J., Mavrouli O., & Ruiz-Carulla R. (2017). Rockfall occurrence and fragmentation. In Advancing Culture of Living with Landslides: Volume 1 ISDR-ICL Sendai Partnerships 2015-2025 (pp. 75-97). Springer International Publishing. DOI 10.1007/978-3-319-59469-9_4

Corominas J., Matas G., & Ruiz-Carulla R. (2019). Quantitative analysis of risk from fragmental rockfalls. Landslides, 16(1), 5-21. DOI 10.1007/s10346-018-1087-9

Crosta G. B., Agliardi F., Frattini P., & Lari S. (2015). Key issues in rock fall modeling, hazard and risk assessment for rockfall protection. In Engineering Geology for Society and Territory-Volume 2: Landslide Processes (pp. 43-58). Springer International Publishing. DOI 10.1007/978-3-319-09057-3_4

Frattini, P., Crosta, G. B., Agliardi, F., Clague, J. J., & Stead, D. (2012). 22-Rockfall characterization and modeling. Landslides: Types, Mechanisms and Modeling; Cambridge University Press: Cambridge, UK, 267-281.

Giacomini A., Buzzi O., Renard B., & Giani G. P. (2009). Experimental studies on fragmentation of rock falls on impact with rock surfaces. International Journal of Rock Mechanics and Mining Sciences, 46(4), 708-715. DOI 10.1016/j.ijrmms.2008.09.007

Gili J. A., Ruiz-Carulla R., Matas G., Moya J., Prades A., Corominas J., ... & Mavrouli O. (2022). Rockfalls: Analysis of the block fragmentation through field experiments. Landslides, 19(5), 1009-1029. DOI 10.1007/s10346-021-01837-9

Guccione D. E., Buzzi O., Thoeni K., Fityus S., & Giacomini A. (2021a). Predicting the fragmentation survival probability of brittle spheres upon impact from statistical distribution of material properties. International Journal of Rock Mechanics and Mining Sciences, 142, 104768. DOI 10.1016/j.ijrmms.2021.104768

Guccione, D. E., Thoeni, K., Fityus, S., Nader, F., Giacomini, A., & Buzzi, O. (2021b). An experimental setup to study the fragmentation of rocks upon impact. Rock Mechanics and Rock Engineering, 54(8), 4201-4223. DOI 10.1007/s00603-021-02501-3

Guccione D. E., Giacomini A., Thoeni K., Fityus S., & Buzzi O. (2023). On the dynamic fragmentation of rock-like spheres: insights into fragment distribution and energy partition. Rock Mechanics and Rock Engineering, 56(2), 847-873. DOI 10.1007/s00603-022-03114-0

Hungr, O. (1988). Engineering evaluation of fragmental rockfall hazard. Proc. of 5th Int. Sympo. on Landslide, Lausanne, 1988, 685-690.

ISRM (1978) Suggested Methods for Determining Tensile Strength of Rock Materials Part 2: Suggested Method for determining indirect tensile strength by the Brazil Test. International Journal of Rock Mechanics and Mining Sciences, 15, 99-103. DOI 10.1016/0148-9062(78)90003-7

ISRM (1979). Suggested methods for determining the uniaxial compressive strength and deformability of rock materials, Int J Rock Mech Min Sci. 16 (2), 135-140. DOI 10.1016/0148-9062(79)91451-7

Khanal M., Schubert W., & Tomas J. (2004). Ball impact and crack propagation–simulations of particle compound material. Granular Matter, 5(4), 177-184. DOI 10.1007/s10035-003-0149-3

Kuruppu M.D., Obara Y. Ayatollahi, M.R. et al. (2014) ISRM-Suggested Method for Determining the Mode I Static Fracture Toughness Using Semi-Circular Bend Specimen. Rock Mech Rock Eng 47, 267–274. DOI 10.1007/s00603-013-0422-7

Lanfranconi C., Frattini P., Sala G., Dattola G., Bertolo D., Sun J., & Crosta G. B. (2023). Accounting for the effect of forest and fragmentation in probabilistic rockfall hazard. Natural Hazards and Earth System Sciences, 23(6), 2349-2363. DOI 10.5194/nhess-23-2349-2023

Lanfranconi C., Frattini P., Agliardi F., Stock G. M., Collins B. D., & Crosta G. (2024). Field evidence and indicators of rockfall fragmentation and implications for mobility. Engineering Geology, 341, 107704. DOI 10.1016/j.enggeo.2024.107704

Lin Q., Cheng Q., Li K., Xie Y., & Wang Y. (2020). Contributions of rock mass structure to the emplacement of fragmenting rockfalls and rockslides: insights from laboratory experiments. Journal of Geophysical Research: Solid Earth, 125(4), e2019JB019296. DOI 10.1029/2019JB019296

Marchelli M., & De Biagi V. (2019). Optimization methods for the evaluation of the parameters of a rockfall fractal fragmentation model. Landslides, 16(7), 1385-1396. DOI 10.1007/s10346-019-01182-y

Marchelli M., De Biagi V., & Peila D. (2021). Reliability-based design of rockfall passive systems height. International Journal of Rock Mechanics and Mining Sciences, 139, 104664. DOI 10.1016/j.ijrmms.2021.104664

Matas G., Lantada N., Corominas J., Gili J., Ruiz-Carulla R., & Prades A. (2020). Simulation of full-scale rockfall tests with a fragmentation model. Geosciences, 10(5), 168. DOI 10.3390/geosciences10050168

Ruiz-Carulla, R., & Corominas, J. (2020). Analysis of rockfalls by means of a fractal fragmentation model. Rock Mechanics and Rock Engineering, 53(3), 1433-1455. DOI 10.1007/s10346-016-0773-8

Scavia C., Barbero M., Castelli M., Marchelli M., Peila D., Torsello G., & Vallero, G. (2020). Evaluating rockfall risk: Some critical aspects. Geosciences, 10(3), 98. DOI 10.3390/geosciences10030098

Schönert K. (2004). Breakage of spheres and circular discs. Powder Technology, 143, 2-18. DOI https://doi.org/10.1016/j.powtec.2004.04.004

Tomas J., Schreier M., Gröger T., & Ehlers S. (1999). Impact crushing of concrete for liberation and recycling. Powder Technology, 105(1-3), 39-51. DOI 10.1016/S0032-5910(99)00116-3

Wang Y., & Tonon F. (2011). Discrete element modeling of rock fragmentation upon impact in rock fall analysis. Rock mechanics and rock engineering, 44, 23-35. DOI 10.1007/s00603-010-0110-9

Wittel F. K., Carmona H. A., Kun F., & Herrmann H. J. (2008). Mechanisms in impact fragmentation. International journal of fracture, 154, 105-117. DOI 10.1007/s10704-008-9267-6

Wu, S. Z., Chau, K. T., & Yu, T. X. (2004). Crushing and fragmentation of brittle spheres under double impact test. Powder Technology, 143, 41-55. DOI 10.1016/j.powtec.2004.04.028

Wu S. Z., & Chau K. T. (2006). Dynamic response of an elastic sphere under diametral impacts. Mechanics of Materials, 38(11), 1039-1060. DOI 10.1016/j.mechmat.2005.08.005

Ye, Y., Zeng, Y., Thoeni, K., & Giacomini, A. (2019). An experimental and theoretical study of the normal coefficient of restitution for marble spheres. Rock Mechanics and Rock Engineering, 52, 1705-1722. DOI 10.1007/s00603-018-1709-5

Ye, Y., Thoeni, K., Zeng, Y., Buzzi, O., & Giacomini, A. (2020). Numerical investigation of the fragmentation process in marble spheres upon dynamic impact. Rock Mechanics and Rock Engineering, 53, 1287-1304. DOI 10.1007/s00603-019-01972-9